

**Bulk sensitive spectroscopy for the valence transition in YbInCu<sub>4</sub>-based compounds**H. Yamaoka,<sup>1</sup> N. Tsujii,<sup>2</sup> K. Yamamoto,<sup>1,3</sup> A. M. Vlaicu,<sup>4,\*</sup> H. Oohashi,<sup>4</sup> H. Yoshikawa,<sup>4</sup> T. Tochio,<sup>5</sup> Y. Ito,<sup>6</sup> A. Chainani,<sup>1</sup> and S. Shin<sup>1,7</sup><sup>1</sup>*Harima Institute, The Institute of Physical and Chemical Research (RIKEN), Sayo, Hyogo 679-5148, Japan*<sup>2</sup>*Quantum Beam Center, National Institute for Materials Science, 1-2-1 Sengen, Tsukuba 305-0047, Japan*<sup>3</sup>*Graduate School of Engineering, Osaka Prefecture University, Sakai, Osaka 599-8531, Japan*<sup>4</sup>*Harima Office, National Institute for Materials Science, Sayo, Hyogo 679-5148, Japan*<sup>5</sup>*Keihanna Interaction Plaza Incorporated, Kyoto 619-0237, Japan*<sup>6</sup>*Institute for Chemical Research, Kyoto University, Uji, Kyoto 611-0011, Japan*<sup>7</sup>*Institute of Solid State Physics, University of Tokyo, Kashiwa, Chiba 277-85817, Japan*

(Received 13 March 2008; revised manuscript received 15 May 2008; published 31 July 2008)

Bulk sensitive x-ray spectroscopy is performed to systematically study the effect of substitution on the valence transition in strongly correlated Yb compounds, such as Y<sub>0.1</sub>Yb<sub>0.9</sub>InCu<sub>4</sub>, YbInCu<sub>4</sub>, and YbIn<sub>0.88</sub>Ag<sub>0.12</sub>Cu<sub>4</sub>, and is compared with complementary magnetic-susceptibility results. High-resolution x-ray absorption spectroscopy with partial fluorescence yields mode and resonant x-ray emission spectroscopy is used to measure the valency change as a function of temperature. The valency change determined from spectroscopy exactly follows the temperature evolution of the magnetic susceptibility. The results confirm first-order transitions in Y<sub>0.1</sub>Yb<sub>0.9</sub>InCu<sub>4</sub> and YbInCu<sub>4</sub>, while YbIn<sub>0.88</sub>Ag<sub>0.12</sub>Cu<sub>4</sub> exhibits a continuous mixed-valence transition. The present results are in agreement with the mean-field Anderson lattice model theory of Goltsev and co-workers [Phys. Rev. B **63**, 155109 (2001); J. Phys.: Condens. Matter **17**, S813 (2005)], which includes the role of local deformations and Kondo volume collapse in the valence transition.

DOI: [10.1103/PhysRevB.78.045127](https://doi.org/10.1103/PhysRevB.78.045127)

PACS number(s): 75.30.Mb, 71.20.Eh, 78.70.En, 78.70.Ck

**I. INTRODUCTION**

The valence transition in *f*-electron systems is one of the most interesting phenomena in strongly correlated materials.<sup>1,2</sup> Among the *f*-electron systems, Ce and Yb are particularly susceptible to mixed-valence behavior due to the small energy gap for the *f*<sup>0</sup>-*f*<sup>1</sup> (Ce<sup>4+</sup>/Ce<sup>3+</sup>) and *f*<sup>13</sup>-*f*<sup>14</sup> (Yb<sup>3+</sup>/Yb<sup>2+</sup>) charge instabilities. A similar condition also holds for the Sm<sup>2+/3+</sup> and Eu<sup>2+/3+</sup> configurations, but the Ce and Yb systems are preferred objects of study due to the simplicity of their *f*<sup>1</sup>-electron or *f*<sup>1</sup>-hole configurations, respectively. YbInCu<sub>4</sub> is very attractive as a typical first-order valence transition system with a critical temperature of  $T_v \sim 40$  K.<sup>3-9</sup> The magnetic susceptibility follows a Curie-Weiss behavior above  $T_v$  with an effective moment close to that of the Yb<sup>3+</sup> ion, while below  $T_v \sim 40$  K, it shows a valency of about 2.8–2.85. Transport results for YbInCu<sub>4</sub> show that, for  $T > T_v$ , the conduction electrons are weakly interacting with the *f* electrons (lower Kondo temperature and higher valence of nearly 3), leading to incoherent Kondo scattering and semimetallic condition. In contrast, for  $T < T_v$ , it is a heavy Fermion Pauli paramagnetic metal. In the low-temperature phase the *f* electrons are strongly hybridized with conduction band states (higher Kondo temperature and mixed valence) and thus quasiparticles near the Fermi surface have a hybrid character and an enhanced mass. The 4*f* occupation number is thus controlled by the Kondo temperature ( $T_K$ ), which is a material-dependent characteristic temperature.

The valence transition in YbInCu<sub>4</sub> is very sensitive to temperature, pressure, and magnetic field.<sup>3,6,10-12</sup> Substitution of Ag on In site, i.e., YbIn<sub>1-x</sub>Ag<sub>x</sub>Cu<sub>4</sub>, results in modifying the first-order discontinuous transition to a continuous

transition and a broad  $T_v$ , which shifts to higher temperature.<sup>13-16</sup> A first-order transition was observed up to  $x=0.1$ , while for  $x=0.3$  it was shown to be a continuous transition with the critical composition being approximately around  $x \sim 0.2$ . Systematic studies have shown that the unit-cell volume does not change significantly up to about  $x = 0.3$  but reduces smoothly for larger  $x$ . Simultaneously, the effective Kondo temperatures, the plasma frequencies, the low-temperature susceptibility, and the Sommerfeld coefficient show little change for  $x \leq 0.3$ , but change significantly for larger  $x$ . On the other hand, substitution of Y on Yb site retains the sharp transition but shifts to a lower temperature.<sup>11,17-19</sup> Hence, YbInCu<sub>4</sub>-based systems with and without substitution provide a very suitable series for a systematic study of the valence transition.

Several scenarios have been proposed to explain the origin of the valence transition in YbInCu<sub>4</sub>: the promotional model,<sup>20,21</sup> the Mott transition (MT) model, or the corrected MT scenario with local-density approximation (LDA) calculation,<sup>22</sup> the Kondo volume collapse (KVC) model based on the single impurity Anderson (SIA) model,<sup>23,24</sup> and LDA calculations with dynamical mean-field theory.<sup>25</sup> The role of geometrical frustration has also been considered to be important for the transition.<sup>26-28</sup> Goltsev and co-workers<sup>29,30</sup> recently developed a mean-field theory taking into account two types of electron-lattice coupling (a local deformation, in addition to the Kondo volume collapse) within the lattice Anderson model framework and successfully explained many experimental results. Hereafter we call this the Goltsev model.<sup>29</sup>

The purpose of this paper is to make a systematic study of the valence transitions in Y<sub>0.1</sub>Yb<sub>0.9</sub>InCu<sub>4</sub>, YbInCu<sub>4</sub>, and YbIn<sub>0.88</sub>Ag<sub>0.12</sub>Cu<sub>4</sub> by bulk sensitive x-ray spectroscopies: the high-resolution x-ray absorption spectroscopy with partial

fluorescence yields mode (PFY-XAS) and resonant x-ray emission spectroscopy (resonant XES) at the Yb  $L_3$  absorption edge. In particular the resonant XES measured in the inelastic mode, also called resonant inelastic x-ray scattering (RIXS), has provided reliable results in a variety of strongly correlated materials.<sup>31–41</sup> A crucial point was the observation of the change in valency with temperature. In this work we study the effect of substitution on the temperature evolution of the mixed valence in detail for  $\text{Y}_{0.1}\text{Yb}_{0.9}\text{InCu}_4$  and  $\text{YbIn}_{0.88}\text{Ag}_{0.12}\text{Cu}_4$  along with the reference material  $\text{YbInCu}_4$ . Using resonant XES measurements at a given incident energy, we obtain the temperature evolution of the valence, while the RIXS and PFY-XAS as a function of the incident photon energy provide the valency.

## II. EXPERIMENTS

Polycrystalline samples of  $\text{Y}_{0.1}\text{Yb}_{0.9}\text{InCu}_4$ ,  $\text{YbInCu}_4$ , and  $\text{YbIn}_{1-x}\text{Ag}_x\text{Cu}_4$  ( $x=0.08, 0.12, 0.22$ ) were prepared by argon arc melting from pure metals and subsequent annealing under vacuum at 1100 K for 20 days. The crystal structure was confirmed and the unit-cell volumes were determined using x-ray diffraction. We confirmed that the unit-cell volume shows negligible change until  $x=0.12$ , indicating a deviation from Vegard's law, as reported earlier.<sup>13,14</sup> The valence transitions were first studied by magnetic-susceptibility measurements. The magnetic susceptibility was measured with a superconducting quantum interference device (SQUID) magnetometer (Quantum design, MPMS5S) at an applied field of 1000 Oe. The x-ray emission spectroscopy was performed at BL15XU undulator beamline of SPring-8.<sup>42</sup> The undulator beam was monochromatized by a water-cooled double crystal monochromator. Energy calibration of the beamline monochromator was performed by using Cu and Ti  $K$  absorption edges. The incident-beam intensity was monitored by a thin Al foil located just before the sample. X-ray emission was measured by Ge 111 double crystal spectrometer with (+,+) geometry.<sup>37,43</sup> The spectrometer has a high energy resolution  $E/\Delta E$  of more than 7000 at the Yb  $L\alpha_1$  energy, where  $E$  is the emitted photon energy. We used a cryostat (Iwatani CRT-M310-OP) to cool down the samples from room temperature to about 17 K. The sample temperature on the holder is measured to an accuracy of about  $\pm 5$  K.

## III. RESULTS AND DISCUSSION

### A. Magnetic susceptibility

Figure 1(a) shows the magnetic-susceptibility data for  $\text{YbIn}_{1-x}\text{Ag}_x\text{Cu}_4$  ( $x=0.0, 0.08, 0.12, 0.22$ ). We obtain a systematic change in the susceptibility as a function of the temperature, which confirms the mixed-valence transition for all the compounds. In Fig. 1(b) we plot the  $1/\chi$  vs  $T$ , showing the similarity in the high-temperature effective moment, where  $1/\chi = T/C - \theta/C$  ( $C$  and  $\theta$  are, respectively, the Curie constant and Weiss temperature). Table I shows the parameter values obtained from a Curie-Weiss fit to the high-temperature susceptibility with the lattice parameters. The Curie constant should be proportional to  $\text{Yb}^{3+}$  magnetic mo-

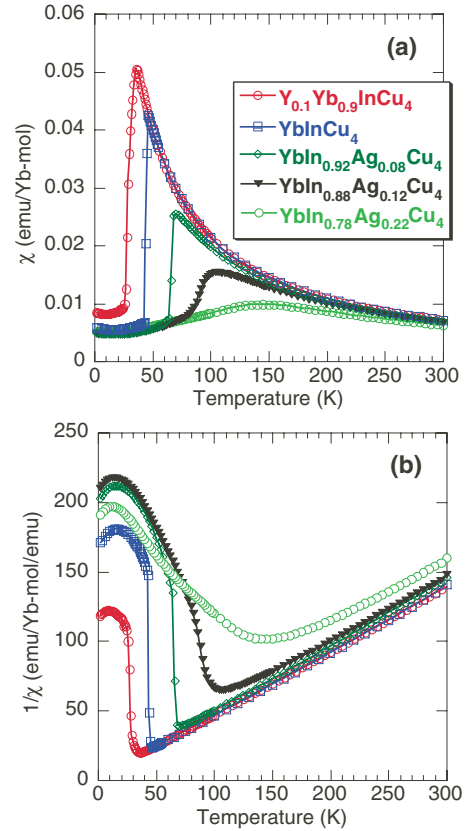


FIG. 1. (Color online) (a) Magnetic susceptibility ( $\chi$ ) of Yb compounds as a function of the temperature ( $T$ ). (b)  $1/\chi$  vs  $T$ .

ment, assuming the nonmagnetic  $\text{Yb}^{2+}$  states. Thus the slope of the linear part of the curves at high temperature in Fig. 2(b) corresponds to the magnetic moment of  $\text{Yb}^{3+}$  component. However the slopes of all curves are almost the same and indicate that the magnetic moments are the same. In Table I the Curie constant does not change, while the Weiss temperature changes from positive to negative values as the Ag doping increases. Normally negative Weiss temperature corresponds to the Ruderman-Kittel-Kasuya-Yosida (RKKY) interaction and stronger antiferromagnetic interaction. However here it is noted that not only the RKKY interaction but also the Kondo effect should be taken into account. From this viewpoint, the shift of the Weiss temperature to the negative value is considered to be due to the increase of the

TABLE I. The parameter values obtained from a Curie-Weiss fit to the high-temperature susceptibility in Fig. 1(b) and the lattice parameters.

Materials	Curie constant (emu K / Yb mol)	Weiss temperature (K)	Lattice parameters (Å)
$\text{Y}_{0.1}\text{Yb}_{0.9}\text{InCu}_4$	2.149	1.4	7.1608
$\text{YbInCu}_4$	2.104	6.6	7.1560
$\text{YbIn}_{0.92}\text{Ag}_{0.08}\text{Cu}_4$	2.070	0.1	7.1545
$\text{YbIn}_{0.88}\text{Ag}_{0.12}\text{Cu}_4$	2.175	-18.6	7.1538
$\text{YbIn}_{0.78}\text{Ag}_{0.22}\text{Cu}_4$	2.155	-42.8	7.1483

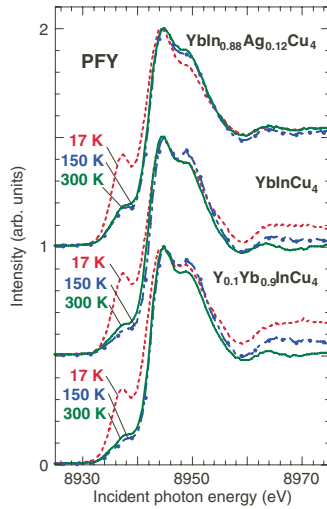


FIG. 2. (Color online) Yb  $L\alpha_1$  PFY spectra as a function of the temperature for  $Y_{0.1}Yb_{0.9}InCu_4$ ,  $YbInCu_4$ , and  $YbIn_{0.88}Ag_{0.12}Cu_4$ .

Kondo temperature with the valence fluctuation at high temperature.<sup>13,14</sup> Indeed, the Kondo temperature of  $YbInCu_4$  at 300 K is much smaller than that of  $YbAgCu_4$ .<sup>13</sup>

For  $YbIn_{1-x}Ag_xCu_4$  ( $x=0.0, 0.08, 0.12, 0.22$ ) the nature of the transition was carefully determined by a plot of  $\chi T$  vs  $T$ . Thus we were able to accurately determine that the  $x=0.0$  and  $0.08$  samples show a first-order transition, while the  $x=0.12$  and  $0.22$  compositions show a continuous transition. Based on the susceptibility results, we selected three samples for x-ray spectroscopic measurements, namely,  $Y_{0.1}Yb_{0.9}InCu_4$ ,  $YbInCu_4$ , and  $YbIn_{0.88}Ag_{0.12}Cu_4$ , as typical materials with the valence transition.

The lattice parameters of the samples measured by x-ray diffraction are also shown in Table I. The change in the lattice parameter for Ag doping is little for  $x \leq 0.12$  and shows small decrease of about 0.1% at  $x=0.22$  compared to  $YbInCu_4$ . For Ag-doping region considered here, the change in the lattice constant does not obey Vegard's law and thus the change in the volume is basically small. Our results agree with those of Sarrao *et al.*<sup>13</sup>

### B. Temperature dependence of PFY and XES

The x-ray absorption spectra were obtained in the PFY-XAS mode. Figure 2 shows Yb  $L\alpha_1$  PFY-XAS spectra as a function of the temperature for  $Y_{0.1}Yb_{0.9}InCu_4$ ,  $YbInCu_4$ , and  $YbIn_{0.88}Ag_{0.12}Cu_4$ . The intensity is normalized to the maximum intensity peak at about 8942 eV. The small peak at 8936 eV and the main peak at around 8942 eV in all the spectra correspond to the  $Yb^{2+}$  and  $Yb^{3+}$  components, respectively. The relative intensity of  $Yb^{2+}$  component increases by decreasing the temperature. We have estimated the valence for quantitative comparison, as will be discussed later. The splitting of  $Yb^{3+}$  peak has been attributed to a crystal field splitting.<sup>4</sup> Upon Ag doping in  $YbInCu_4$ , the peak splitting becomes less distinct at  $T=17$  K and suggests a decrease in the strength of the crystal field splitting.

We also measured the PFY-XAS spectra for Cu  $K\alpha_1$  emission at Cu  $K$  absorption edge (not shown here). The results

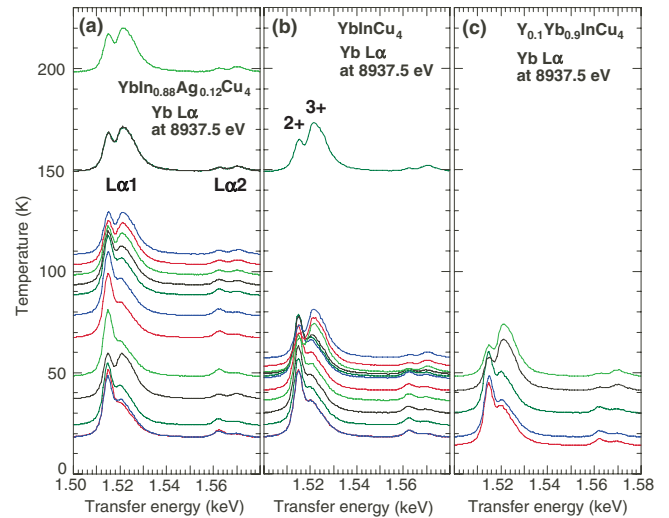


FIG. 3. (Color online) Yb  $L\alpha$  photon emission spectra at the incident photon energy of 8937.5 eV as a function of the temperature for (a)  $Y_{0.1}Yb_{0.9}InCu_4$ , (b)  $YbInCu_4$ , and (c)  $YbIn_{0.88}Ag_{0.12}Cu_4$ . Position of base line of each spectrum scales to the temperature of the vertical axis.

indicate negligible differences among the Yb compounds at 17 and 250 K and the spectra are similar to the PFY-XAS spectrum of Cu metal, typical of an intermetallic compound.

Yb  $L\alpha$  resonant x-ray emission spectra at the incident photon energy of 8937.5 eV as a function of the temperature are shown in Fig. 3 for  $Y_{0.1}Yb_{0.9}InCu_4$ ,  $YbInCu_4$ , and  $YbIn_{0.88}Ag_{0.12}Cu_4$ . The transfer energy is the difference between the incident and emitted photon energies. The peaks at low- and high-energy sides of  $L\alpha_1$  are  $Yb^{2+}$  and  $Yb^{3+}$  components, respectively. The incident photon energy was chosen to observe both components of  $Yb^{2+}$  and  $Yb^{3+}$  with equivalent intensity, where the fluorescence contribution could be ignored. The intensity across the valence transition temperature in  $YbIn_{0.88}Ag_{0.12}Cu_4$  changes gradually, while that in  $YbInCu_4$  and  $Y_{0.1}Yb_{0.9}InCu_4$  is rapid as a function of temperature. In order to carefully investigate the temperature dependence of the spectral changes across the transitions, we have carried out curve fits to the spectra shown in Fig. 3.<sup>37</sup>

### C. Resonant inelastic x-ray scattering

The RIXS gives a quantification of the valence as well as information about the electronic state occupancy and localization of  $4f$  states, as was recently shown for the  $\alpha$ - $\gamma$  transition in cerium.<sup>36</sup> We measured the RIXS spectra as a function of the incident photon energies for  $Y_{0.1}Yb_{0.9}InCu_4$  (at 17 K),  $YbInCu_4$  (at 17 K), and  $YbIn_{0.88}Ag_{0.12}Cu_4$  (at 17 and 148 K), corresponding to particular energies in the PFY spectra, as shown in Fig. 4. In RIXS spectra the peak energy position of the Raman component does not change and the fluorescence component is proportional to the transfer energy.<sup>44</sup> Below the absorption edge the Raman component is clearly observed and two distinct peaks correspond to two valence states of  $Yb^{2+}$  and  $Yb^{3+}$ , while far above the absorption edge the fluorescence component is mainly observed.

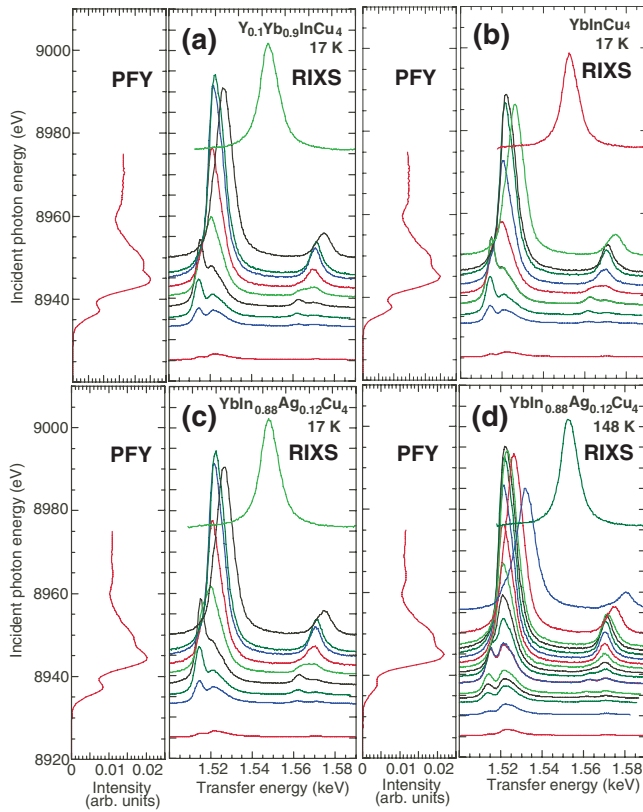


FIG. 4. (Color online) Resonant inelastic-scattering spectra as a function of the incident photon energies for (a)  $\text{Y}_{0.1}\text{Yb}_{0.9}\text{InCu}_4$  (at 17 K), (b)  $\text{YbInCu}_4$  (at 17 K), (c)  $\text{YbIn}_{0.88}\text{Ag}_{0.12}\text{Cu}_4$  (at 17 K), and (d)  $\text{YbIn}_{0.88}\text{Ag}_{0.12}\text{Cu}_4$  (at 148 K). The vertical scale of the right panel corresponds to x-ray intensity. Position of base line of each spectrum in the right panel scales to the energy of the left panel.

We separate the contribution of the fluorescence component for the spectra in Fig. 4 to quantify the value of the valence from the Raman component through a curve-fitting procedure.<sup>37</sup> Figure 5 shows the results: the change in the intensity of  $\text{Yb}^{2+}$  and  $\text{Yb}^{3+}$  components is plotted along with the PFY spectra. At 17 K the features among the three compounds show small differences, while at 148 K large changes can be seen for  $\text{YbIn}_{0.88}\text{Ag}_{0.12}\text{Cu}_4$ .

We summarize the values of the mean valence in Fig. 6, estimated by integrating the area of each charge state shown in Fig. 5 together with the plot of  $\chi T$  for the three compounds, confirming that the spectral intensity ratio exactly follows the  $\chi T$  changes around the critical temperature. The mean valence is defined to be  $v = 2 + I(3+) / [I(2+) + I(3+)]$ , where  $I(n+)$  is the intensity of  $\text{Yb}^{n+}$  component. The intensity of  $\text{Yb}^{2+}$  is basically small compared to that of  $\text{Yb}^{3+}$ , thus the valence is near the value of 3. In Fig. 6 we also plot the temperature dependence of the intensity ratio,  $\text{Yb}^{3+}$  to  $\text{Yb}^{2+}$  derived from the curve fitting for the data in Fig. 3, to see the relative change in the valence. However these ratios do not give the values of the mean valences. Thus in Fig. 6, we include the data transformed from the ratio by adjusting the value of the ratio to the mean valence of the PFY measurement in order to see the detailed behavior of the valency around the critical temperatures. In the high-temperature phase the valence is about 2.95 and in the low-temperature

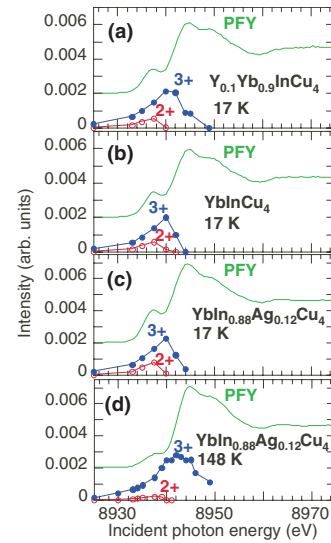


FIG. 5. (Color online) Incident photon energy dependence of each charge state obtained through the curve-fitting procedure for the RIXS spectra of Fig. 4 with the PFY spectra for  $\text{Y}_{0.1}\text{Yb}_{0.9}\text{InCu}_4$ ,  $\text{YbInCu}_4$ , and  $\text{YbIn}_{0.88}\text{Ag}_{0.12}\text{Cu}_4$ .

phase below the transition it becomes about 2.8–2.85 for the three compounds. Thus small changes in the valence of about 0.1–0.15 cause significant change in the material character.

The critical temperatures of the susceptibility and the  $\text{Yb} \text{La}_1$  ratio at the phase transition are estimated to be centered about 30 K for  $\text{Y}_{0.1}\text{Yb}_{0.9}\text{InCu}_4$ , 44 K for  $\text{YbInCu}_4$ , and a broad transition between about 85 and 105 K for  $\text{YbIn}_{0.88}\text{Ag}_{0.12}\text{Cu}_4$ . The change in the lattice constants, susceptibility, specific heat, and reflectivity for  $\text{YbInCu}_4$  showed

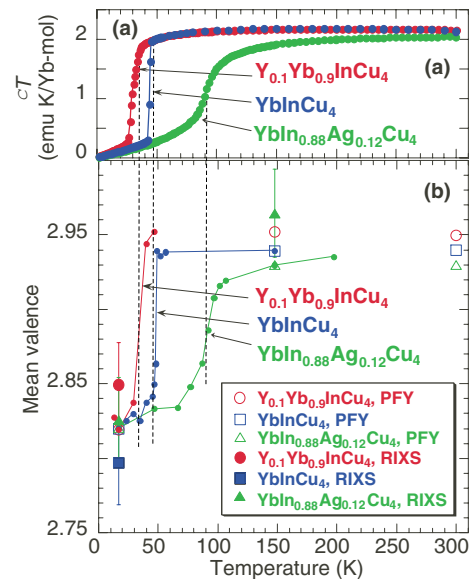


FIG. 6. (Color online) (a)  $\chi T$  as a function of temperature. (b) The mean valence estimated from the data of Fig. 5 (open and closed points) for  $\text{Y}_{0.1}\text{Yb}_{0.9}\text{InCu}_4$ ,  $\text{YbInCu}_4$ , and  $\text{YbIn}_{0.88}\text{Ag}_{0.12}\text{Cu}_4$ . The solid lines correspond to the valence converted from the intensity ratio,  $\text{Yb}^{3+}$  to  $\text{Yb}^{2+}$  derived from the data in Fig. 3, by adjusting these ratios to the values of the valences obtained from the PFY measurement.

the transition temperature of about  $T_v=40-46$  K,<sup>45-48</sup> consistent with our measurements. The transition temperatures of the resonant XES agree well within the accuracy of the measured sample temperature. Recent measurements with photoelectron spectroscopy (PES) for YbInCu<sub>4</sub> showed that the critical temperature  $T_v$  is modified on the surface, while bulk sensitive measurements are consistent with thermodynamic measurements.<sup>49-51</sup> Surface sensitive PES measurements for YbInCu<sub>4</sub> indicated that the transition temperature in such spectra was higher than  $T_v$ .<sup>51,52</sup> Yoshikawa *et al.*<sup>52</sup> suggested the effect of the surface sensitivity of the PES based on the following: Yb valence of outermost layer is divalent but gets to be nearly trivalent in the bulk. The ionic radius of Yb<sup>2+</sup> ion is about 10% as large as that of Yb<sup>3+</sup> ion and the lattice constant at the surface is larger compared to that of the bulk. Subsequently the transition from trivalent to divalent is easy to take place at the surface due to the larger space. Our results of the RIXS clearly show that transition temperatures are not only consistent with bulk magnetic-susceptibility measurements but can also distinguish between first-order and continuous transitions.

Sato *et al.*<sup>53</sup> showed slightly smaller values that the Yb valence changed from about 2.9 to 2.74 at the transition for YbInCu<sub>4</sub> by hard x-ray photoelectron spectroscopy (HAXPES) with 5.95 keV photons upon decreasing the temperature. The XAS at Yb  $L_3$  absorption edge for YbInCu<sub>4</sub> showed the valence of about 2.8-2.9.<sup>3</sup> In the RIXS for YbInCu<sub>4</sub> Dallera *et al.*<sup>31</sup> showed that  $1-\langle n_f \rangle$  was 0.13 at 15 K and 0.065 at 300 K, corresponding to the valences of 2.87 (15 K) and 2.935 (300 K), where  $\langle n_f \rangle$  was  $4f$  hole number. These values are almost the same as in the present measurements. Recently Moreschini *et al.*<sup>32</sup> compared the valencies derived from the RIXS to those from HAXPES for Yb compounds and showed that the RIXS and XAS valencies were slightly higher than the HAXPES values. They suggested that this difference is due to the influence from the near-surface disorder in HAXPES.

#### D. Mechanism of the valence transition

Gunnarsson and Schönhammer<sup>54</sup> showed the relation of  $n_f/(1-n_f)=N_f\Delta/T_K$  and  $T_K=D \exp(-\pi\epsilon_f/N_f\Delta)$  based on the SIA model, where  $n_f$ ,  $\Delta$ ,  $N_f$ ,  $D$ , and  $\epsilon_f$  are the hole number of Yb, the hybridization strength between  $4f$  and conduction band, the degeneracy of  $f$  level, the effective bandwidth, and the energy of the  $f$  level to the Fermi energy, respectively.<sup>55</sup> Left part of the first equation becomes smaller if the hole number decreases. On the other hand,  $T_K$  changes exponentially for the change in the  $N_f\Delta$ . Thus the decrease of the hole number causes the large increase of  $T_K$ . Our experimental result in Fig. 6 shows that the decrease of the hole number occurs at  $T_v$  on decreasing temperature, while  $T_K$  increases for the low-temperature phase. This shows that the SIA model describes the change in the valence qualitatively.

The electronic states at the Fermi level play an important role in Yb compounds exhibiting mixed valence. Sato *et al.*<sup>56</sup> observed a considerable enhancement and a small energy shift of Yb<sup>2+</sup>  $4f_{7/2}$  for YbInCu<sub>4</sub> by HAXPES on decreasing the temperature. If we assume  $4f_{7/2}$  as the Kondo peak, the

increase in this peak corresponds to the increase in the Kondo temperature. The value of the peak shift was, however, too small ( $\sim 3$  meV) compared to the value expected ( $\sim 32$  meV) from the SIA model.

Recently the role of frustration as an origin of the valence transition has also been proposed for the series  $R\text{InCu}_4$  with  $R=\text{Gd-Tm}$  and for  $\text{YbIn}_{1-x}\text{M}_x\text{Cu}_4$  with  $M=\text{Cd}$  and  $\text{Rh}$ .<sup>27,28</sup> Ramirez<sup>26</sup> indicated that the system was moderately frustrated for  $F\sim 3$ , frustrated for  $F\geq 5$ , and strongly frustrated for  $F\geq 10$ , where the frustration parameter  $F$  was the ratio of Curie-Weiss temperature to Néel temperature ( $F=-\Theta/T_N$ ). Fritsch *et al.*<sup>28</sup> showed that the frustration parameter increased upon decreasing the Rh concentration  $x$  in  $\text{YbIn}_{1-x}\text{Rh}_x\text{Cu}_4$ . Thus they concluded that the geometrical frustration might be a driving factor for  $R\text{InCu}_4$  ( $R$ —rare earth).<sup>27,28</sup>

In the KVC model the change in the characteristic energy (Kondo temperature) due to change in the volume is the origin of the valence fluctuation and thus the driving force of the transition is the volume collapse. For the  $\gamma$ -Ce to  $\alpha$ -Ce transition, Cornelius *et al.*<sup>14</sup> confirmed the applicability of the KVC model through the estimation of the Grüneisen parameter. In YbInCu<sub>4</sub>, however, they estimated unrealistically large Grüneisen parameter. Cornelius *et al.*<sup>14</sup> considered the scenario for the valence transition based on a quasigap or region of low density of states (DOS), existing just above the Fermi level. The presence of the quasigap makes the Kondo temperature sensitive to the position of the Fermi level, showing the importance of the DOS dependence rather than the change in volume. In another related series of Ce-based mixed-valence transition compounds  $\text{CeNi}_{1-x}\text{Co}_x\text{Sn}$ , Adroja *et al.*<sup>57</sup> showed nonapplicability of the KVC model. We recently reported the PFY-XAS, RIXS, and resonant photoelectron spectroscopy for  $\text{CeNi}_{1-x}\text{Co}_x\text{Sn}$ .<sup>38</sup> The results indicated a similar scenario as above that the fine tuning of the Fermi-level position results in a large change in the hybridization and the Kondo temperature with a small change in the volume. We also discussed similar anomalous behavior of the Grüneisen parameter in  $\text{YbCu}_{5-x}\text{Al}_x$ .<sup>39</sup> The conclusions are, however, at variance with that of Svechkarov *et al.*<sup>10</sup> for YbInCu<sub>4</sub>. Cornelius *et al.*<sup>14</sup> claimed that the value of the Grüneisen parameter did not explain the large change in the Kondo temperature. Another problem was the negative sign of the Grüneisen parameter.

Goltsev *et al.*<sup>29,30</sup> successfully explained many experimental results for Ce- and Yb-based valence transitions, including the change in sign of the Grüneisen parameter, based on a lattice Anderson model. In particular they considered two mechanisms of electron-lattice coupling: volume dependence of  $c$ - $f$  hybridization and local deformations produced by ionic radius fluctuations of rare-earth ions accompanying valence fluctuation.<sup>29,30</sup> It was found that the Coulomb interaction enhanced the exchange interaction between  $f$  and conduction-band electron spins and was the driving force of the phase transition. In the Goltsev model<sup>29</sup> the origin of the phase transition is still the Kondo effect.

In our experiments it is clear that the small change in the valence of about 0.1-0.15 at  $T_v$  corresponds to the changes in magnetic character for the three compounds. The change in volume was very small as described above in YbInCu<sub>4</sub>.

Also, for  $\text{YbIn}_{1-x}\text{Ag}_x\text{Cu}_4$ , the unit-cell volume changed by substitution does not follow the Vegard law, but the system undergoes a change from first order to a continuous transition. Thus the main question was that why do the physical properties of  $\text{YbInCu}_4$  and  $\text{YbIn}_{1-x}\text{Ag}_x\text{Cu}_4$  change significantly, despite the small change in the valence and volume. In this point of view the simple KVC model based on the simple SIA model is not enough to explain the origin of the valence transition for  $\text{YbInCu}_4$  and the substituted  $\text{YbIn}_{1-x}\text{Ag}_x\text{Cu}_4$  systems, although it is applicable for  $\gamma$  to  $\alpha$  transition in Ce metal.

The observed spectral changes in  $\text{Y}_{0.1}\text{Yb}_{0.9}\text{InCu}_4$ ,  $\text{YbInCu}_4$ , and  $\text{YbIn}_{0.88}\text{Ag}_{0.12}\text{Cu}_4$  are consistent with the Goltsev model.<sup>29</sup> In their model, for the high-temperature phase,  $f$  electrons are strongly localized and the valence is 3. While for the low-temperature phase, the  $c$ - $f$  hybridization is stronger with heavy electrons and the valence decreases by 0.24 in  $\text{YbAgCu}_4$ . In the Goltsev model<sup>29</sup> Yb systems in the low-temperature mixed-valence phase, the valency change is negative, the volume change is positive, and the system gains energy. At present the Goltsev model<sup>29</sup> well describes our experimental results. However we note that the agreement is only qualitative and we need more quantitative calculation to compare our data with the model. Further theoretical study may be required to understand the mechanism of the valence transition. Finally, in the Ag-doped system the Kondo effect is weaker compared to  $\text{YbInCu}_4$  because the change in the volume is smaller at  $T \sim T_c$ .<sup>14</sup> This is attributed to the screening of the on-site Coulomb energy in  $\text{YbIn}_{0.88}\text{Ag}_{0.12}\text{Cu}_4$  on substituting Ag and results in a crossover from a first order to a continuous transition.

#### IV. CONCLUSION

We performed PFY-XAS and RIXS measurements on  $\text{Y}_{0.1}\text{Yb}_{0.9}\text{InCu}_4$ ,  $\text{YbInCu}_4$ , and  $\text{YbIn}_{0.88}\text{Ag}_{0.12}\text{Cu}_4$  to study the temperature-induced valence transition systematically. The bulk sensitive spectroscopy demonstrates a detailed temperature evolution of the resonant XES and the valence change exactly follows the temperature evolution of magnetic susceptibility around the critical temperature. The mechanism of the phase transition in  $\text{YbInCu}_4$  system has been an open question for a long time. We compared the experimental results with different theoretical models which were proposed to explain this striking phenomenon. The SIA model is not enough to explain the present results regarding the origin of the valence transition for  $\text{YbInCu}_4$  and  $\text{YbIn}_{1-x}\text{Ag}_x\text{Cu}_4$  systems but is consistent with the Goltsev model<sup>29</sup> which includes the role of local deformations and Kondo volume collapse in the valence transition. Although at present the Goltsev model<sup>29</sup> well describes our experimental results, further theoretical study may be required. In the Ag-doped system the Kondo effect is weaker compared to  $\text{YbInCu}_4$ , and the transition becomes continuous due to an effective screening of the on-site Coulomb energy. These behaviors may be related to the changes in the DOS near the Fermi level, where small changes in such electronic states can strongly affect the phase transition.

#### ACKNOWLEDGMENTS

The experiments were performed at BL15XU (under the approval of NIMS through Proposal No. 2005B4700) of SPring-8. This work was partly supported by Grant-in-Aid for Scientific Research under Grant No. 19740221.

\*Present address: National Institute of Material Physics, Bucharest-Magurele 077125, Romania.

<sup>1</sup>C. M. Varma, *Rev. Mod. Phys.* **48**, 219 (1976).

<sup>2</sup>P. Strange, A. Svane, W. M. Temmerman, Z. Szotek, and H. Winter, *Nature (London)* **399**, 756 (1999).

<sup>3</sup>I. Felner and I. Nowik, *Phys. Rev. B* **33**, 617 (1986).

<sup>4</sup>I. Felner, I. Nowik, D. Vaknin, U. Potzel, J. Moser, G. M. Kalvius, G. Wortmann, G. Schmiester, G. Hilscher, E. Gratz, C. Schmitzer, N. Pillmayr, K. G. Prasad, H. de Waard, and H. Pinto, *Phys. Rev. B* **35**, 6956 (1987).

<sup>5</sup>I. Nowik, I. Felner, J. Voiron, J. Beille, A. Najib, E. du Tremolet de Lacheisserie, and G. Gratz, *Phys. Rev. B* **37**, 5633 (1988).

<sup>6</sup>J. L. Sarrao, *Physica B (Amsterdam)* **259-261**, 128 (1999), and references cited therein.

<sup>7</sup>K. Kojima, Y. Nakai, T. Suzuki, H. Asano, F. Izumi, T. Fujita, and T. Hihara, *J. Phys. Soc. Jpn.* **59**, 792 (1990).

<sup>8</sup>B. Kindler, D. Finsterbusch, R. Graf, F. Ritter, W. Assmus, and B. Luthi, *Phys. Rev. B* **50**, 704 (1994).

<sup>9</sup>T. Koyama, M. Matsumoto, T. Tanaka, H. Ishida, T. Mito, S. Wada, and J. L. Sarrao, *Phys. Rev. B* **66**, 014420 (2002).

<sup>10</sup>I. V. Svehkarev, A. S. Panfilov, S. N. Dolja, H. Nakamura, and M. Shiga, *J. Phys.: Condens. Matter* **11**, 4381 (1999).

<sup>11</sup>W. Zhang, N. Sato, K. Yoshimura, A. Mitsuda, T. Goto, and K.

Kosuge, *Phys. Rev. B* **66**, 024112 (2002).

<sup>12</sup>N. V. Mushnikov, T. Goto, E. V. Rozenfeld, K. Yoshimura, W. Zhang, M. Yamada, and H. Kageyama, *J. Phys.: Condens. Matter* **15**, 2811 (2003).

<sup>13</sup>J. L. Sarrao, C. D. Immer, C. L. Benton, Z. Fisk, J. M. Lawrence, D. Mandrus, and J. D. Thompson, *Phys. Rev. B* **54**, 12207 (1996).

<sup>14</sup>A. L. Cornelius, J. M. Lawrence, J. L. Sarrao, Z. Fisk, M. F. Hundley, G. H. Kwei, J. D. Thompson, C. H. Booth, and F. Bridges, *Phys. Rev. B* **56**, 7993 (1997).

<sup>15</sup>M. Očko, J. L. Sarrao, and Ž. Simek, *J. Magn. Magn. Mater.* **284**, 43 (2004).

<sup>16</sup>J. N. Hancock, T. McKnew, Z. Schlesinger, J. L. Sarrao, and Z. Fisk, *Phys. Rev. B* **73**, 125119 (2006).

<sup>17</sup>A. Mitsuda, T. Goto, K. Yoshimura, W. Zhang, N. Sato, K. Kosuge, and H. Wada, *Phys. Rev. Lett.* **88**, 137204 (2002).

<sup>18</sup>M. Očko, J. L. Sarrao, I. Aviani, Dj. Drobac, I. Zivković, and M. Prester, *Phys. Rev. B* **68**, 075102 (2003).

<sup>19</sup>J. K. Freericks and V. Zlatic, *Phys. Status Solidi B* **236**, 265 (2003).

<sup>20</sup>L. M. Falicov and J. C. Kimball, *Phys. Rev. Lett.* **22**, 997 (1969).

<sup>21</sup>R. Ramirez and L. M. Falicov, *Phys. Rev. B* **3**, 2425 (1971).

- <sup>22</sup>B. Johansson, *Philos. Mag.* **30**, 469 (1974); B. Johansson, I. A. Abrikosov, M. Alden, A. V. Ruban, and H. L. Skriver, *Phys. Rev. Lett.* **74**, 2335 (1995).
- <sup>23</sup>J. W. Allen and R. M. Martin, *Phys. Rev. Lett.* **49**, 1106 (1982); J. W. Allen and L. Z. Liu, *Phys. Rev. B* **46**, 5047 (1992); L. Z. Liu, J. W. Allen, O. Gunnarsson, N. E. Christensen, and O. K. Andersen, *ibid.* **45**, 8934 (1992).
- <sup>24</sup>M. Lavagna, C. Lacroix, and M. Cyrot, *Phys. Lett.* **90A**, 210 (1982).
- <sup>25</sup>A. K. McMahan, K. Held, and R. T. Scalettar, *Phys. Rev. B* **67**, 075108 (2003).
- <sup>26</sup>A. P. Ramirez, *Annu. Rev. Mater. Sci.* **24**, 453 (1994).
- <sup>27</sup>V. Fritsch, J. D. Thompson, and J. L. Sarrao, *Phys. Rev. B* **71**, 132401 (2005).
- <sup>28</sup>V. Fritsch, J. D. Thompson, S. Bobev, and J. L. Sarrao, *Phys. Rev. B* **73**, 214448 (2006).
- <sup>29</sup>A. V. Goltsev and G. Bruls, *Phys. Rev. B* **63**, 155109 (2001).
- <sup>30</sup>A. V. Goltsev, and M. M. Abd-Elmeguid, *J. Phys.: Condens. Matter* **17**, S813 (2005).
- <sup>31</sup>C. Dallera, M. Grioni, A. Shukla, G. Vankó, J. L. Sarrao, J.-P. Rueff, and D. L. Cox, *Phys. Rev. Lett.* **88**, 196403 (2002).
- <sup>32</sup>L. Moreschini, C. Dallera, J. J. Joyce, J. L. Sarrao, E. D. Bauer, V. Fritsch, S. Bobev, E. Carpena, S. Huotari, G. Vankó, G. Monaco, P. Lacovig, G. Panaccione, A. Fondacaro, G. Paolicelli, P. Torelli, and M. Grioni, *Phys. Rev. B* **75**, 035113 (2007).
- <sup>33</sup>C. Dallera, E. Annese, J.-P. Rueff, A. Palenzona, G. Vankó, L. Braicovich, A. Shukla, and M. Grioni, *Phys. Rev. B* **68**, 245114 (2003).
- <sup>34</sup>J.-P. Rueff, J.-P. Itié, M. Taguchi, C. F. Hague, J.-M. Mariot, R. Delaunay, J.-P. Kappler, and N. Jaouen, *Phys. Rev. Lett.* **96**, 237403 (2006).
- <sup>35</sup>J.-P. Rueff, L. Journel, P.-E. Petit, and F. Farges, *Phys. Rev. B* **69**, 235107 (2004).
- <sup>36</sup>J.-P. Rueff, C. F. Hague, J.-M. Mariot, L. Journel, R. Delaunay, J.-P. Kappler, G. Schmerber, A. Derory, N. Jaouen, and G. Krill, *Phys. Rev. Lett.* **93**, 067402 (2004).
- <sup>37</sup>H. Yamaoka, M. Taguchi, A. M. Vlaicu, H. Ohashi, Y. Yokoi, D. Horiguchi, T. Tochio, Y. Ito, K. Kawatsura, K. Yamamoto, A. Chainani, S. Shin, M. Shiga, and H. Wada, *J. Phys. Soc. Jpn.* **75**, 034702 (2006).
- <sup>38</sup>H. Yamaoka, N. Tsujii, K. Yamamoto, H. Ohashi, A. M. Vlaicu, K. Kunitani, K. Uotani, D. Horiguchi, T. Tochio, Y. Ito, and S. Shin, *Phys. Rev. B* **76**, 075130 (2007).
- <sup>39</sup>K. Yamamoto, H. Yamaoka, N. Tsujii, A. M. Vlaicu, H. Ohashi, S. Sakakura, T. Tochio, Y. Ito, A. Chainani, and S. Shin, *J. Phys. Soc. Jpn.* **76**, 124705 (2007).
- <sup>40</sup>H. Yamaoka, H. Ohashi, I. Jarrige, T. Terashima, Y. Zou, H. Mizota, S. Sakakura, T. Tochio, Y. Ito, E. Y. Sherman, and A. Kotani, *Phys. Rev. B* **77**, 045135 (2008).
- <sup>41</sup>H. Yamaoka, N. Tsujii, H. Ohashi, D. Nomoto, I. Jarrige, K. Takahiro, K. Ozaki, K. Kawatsura, and Y. Takahashi, *Phys. Rev. B* **77**, 115201 (2008).
- <sup>42</sup>A. Nisawa, M. Okui, N. Yagi, T. Mizutani, H. Yoshikawa, and S. Fukushima, *Nucl. Instrum. Methods Phys. Res. A* **497**, 563 (2003).
- <sup>43</sup>D. Horiguchi, K. Yokoi, H. Mizota, S. Sakakura, H. Ohashi, Y. Ito, T. Tochio, A. M. Vlaicu, H. Yoshikawa, S. Fukushima, H. Yamaoka, and T. Shoji, *Radiat. Phys. Chem.* **75**, 1830 (2006).
- <sup>44</sup>T. Åberg and B. Crasemann, in *Resonant Anomalous X-ray Scattering Theory and Application*, edited by G. Materlik, C. J. Sparks, and K. Fischer (Elsevier, Amsterdam, 1994), p. 431.
- <sup>45</sup>J. M. Lawrence, G. H. Kwei, J. L. Sarrao, Z. Fisk, D. Mandrus, and J. D. Thompson, *Phys. Rev. B* **54**, 6011 (1996).
- <sup>46</sup>J. L. Sarrao, A. P. Ramirez, T. W. Darling, F. Freibert, A. Migliori, C. D. Immer, Z. Fisk, and Y. Uwatoko, *Phys. Rev. B* **58**, 409 (1998).
- <sup>47</sup>V. N. Lazukov, A. S. Ivanov, F. Ritter, P. A. Alekseev, W. Assmus, I. P. Sadikov, and N. N. Tiden, *Physica B (Amsterdam)* **350**, E139 (2004).
- <sup>48</sup>H. Okamura, T. Michizawa, T. Nanba, and T. Ebihara, *Phys. Rev. B* **75**, 041101(R) (2007).
- <sup>49</sup>H. Sato, K. Shimada, M. Arita, K. Hiraoka, K. Kojima, Y. Takeda, K. Yoshikawa, M. Sawada, M. Nakatake, H. Namatame, M. Taniguchi, Y. Takata, E. Ikenaga, S. Shin, K. Kobayashi, K. Tamasaku, Y. Nishino, D. Miwa, M. Yabashi, and T. Ishikawa, *Phys. Rev. Lett.* **93**, 246404 (2004).
- <sup>50</sup>F. Reinert, R. Claessen, G. Nicolay, D. Ehm, S. Hufner, W. P. Ellis, G.-H. Gweon, J. W. Allen, B. Kindler, and W. Assmus, *Phys. Rev. B* **58**, 12808 (1998).
- <sup>51</sup>S. Schmidt, S. Hufner, F. Reinert, and W. Assmus, *Phys. Rev. B* **71**, 195110 (2005).
- <sup>52</sup>K. Yoshikawa, H. Sato, M. Arita, Y. Takeda, K. Hiraoka, K. Kojima, K. Tsuji, H. Namatame, and M. Taniguchi, *Phys. Rev. B* **72**, 165106 (2005).
- <sup>53</sup>H. Sato, K. Shimada, M. Arita, Y. Takeda, M. Sawada, M. Nakatake, K. Yoshikawa, H. Namatame, Y. Takata, K. Kobayashi, E. Ikenaga, S. Shin, M. Yabashi, D. Miwa, Y. Nishino, K. Tamasaku, T. Ishikawa, K. Hiraoka, K. Kojima, and M. Taniguchi, *Physica B (Amsterdam)* **351**, 298 (2004).
- <sup>54</sup>O. Gunnarsson and K. Schönhammer, *Phys. Rev. B* **28**, 4315 (1983).
- <sup>55</sup>F. Patthey, J.-M. Imer, W.-D. Schneider, H. Beck, Y. Baer, and B. Delley, *Phys. Rev. B* **42**, 8864 (1990).
- <sup>56</sup>H. Sato, K. Hiraoka, M. Taniguchi, Y. Nishikawa, F. Nagasaki, H. Fujino, Y. Takeda, M. Arita, K. Shimada, H. Namatame, A. Kimura, and K. Kojima, *J. Phys.: Condens. Matter* **14**, 4445 (2002).
- <sup>57</sup>D. T. Adroja, Y. Echizen, T. Takabatake, Y. Matsumoto, T. Suzuki, T. Fujita, and B. D. Rainford, *J. Phys.: Condens. Matter* **11**, 543 (1999).